solvent was evaporated, and additional Et_2O (25 mL) added to the solid residue. This cycle was repeated three times. An IR analysis of the material obtained showed that ca. 50% of **3** had been converted to **5**. The two products were separated by fractional crystallization as described above.

Preparation of Ni[η^2-C(NBu^t)CH$_3$](NC$_4$H$_2$Me$_2$)(PMe$_3$) (8). CNBu^t (0.23 mL, 2 mmol) was added to a cold (-40 °C), stirred, orange solution of Ni(Me)(NC$_4$H$_2$Me$_2$)(PMe$_3$)$_2$ (0.69 g, 2 mmol) in Et_2O (40 mL). The reaction mixture was allowed to reach room temperature and further stirred for 5 h, when the solution changed to red. After removal of the volatiles in vacuo, compound **8** was obtained as red crystals (45% yield) by extraction of the residue with a mixture of petroleum ether–Et_2O (2:1, 30 mL), filtration, concentration, and cooling at -30 °C.

The red complexes **7** and **10** were obtained in ca. 40% yield following a similar procedure. However, in the preparation of the yellow (trimethylsilyl)methyl derivative **9** traces of humidity should be very carefully avoided as water easily converts compound **9** into the analogous methyl derivative **8**. To purposefully achieve this transformation, to a solution of **9** in acetone was added one drop of water. After it was stirred for 30 min at room temperature, the solution changed from yellow to red. NMR spectroscopy shows the presence of compound **8** in the reaction mixture from which it can be isolated by crystallization from petroleum ether–Et_2O.

Synthesis of CpNi[η^1-C(NBu^t)CH$_3$]PMe$_3$ (11). Complex **1** (0.53 g, 1.5 mmol) was dissolved in Et_2O (30 mL), and the resulting solution cooled at -40 °C and reacted with 1 equiv of NaCp (2 mL of a 0.8 N solution in THF) added via syringe. The mixture was stirred for 3 h at room temperature, when the color changed to dark red. The volatiles were removed in vacuo, and the residue extracted with petroleum ether–Et_2O (1:1). Dark red crystals were obtained in 60% yield by centrifugation, partial removal of the solvent, and cooling at -30 °C.

Following a similar procedure, compound **12** was obtained as dark red crystals in 70% yield (from petroleum ether at -30 °C).

Preparation of Ni[η^1-C(NBu^t)Me](S$_2$CNMe$_2$)PMe$_3$ (13). An excess of dried, finely ground NaS_2CNMe_2 (0.21 g, 1.5 mmol) was added as a solid to a stirred solution of complex **1** (0.34 g, 1 mmol) in THF (30 mL). After stirring for 12 h at room temperature, the mixture was taken to dryness and the residue extracted with petroleum ether–Et_2O (1:2, 30 mL). Filtration, concentration of the resulting solution, and cooling at -30 °C furnished the desired product as red crystals in 75% yield.

Synthesis of [Ni(C(NHBu^t)Me)Cl(PMe$_3$)$_2$]BF$_4$ (14b). To a stirred, cold (-40 °C) solution of complex **1** (0.34 g, 1 mmol) in Et_2O (30 mL) was added 1.5 equiv of HBF_4 (0.3 mL of a 35% solution in water). The formation of a precipitate was noted, and the resulting suspension was stirred at room temperature for 30 min. The yellow product was filtered and dried in vacuo to afford **14b** in almost quantitative yield. An analytical sample was obtained, in the form of yellow-orange crystals upon crystallization of the crude product from toluene–CH_2Cl_2 at -40 °C.

By adding aqueous solutions of HCl and HNO_3 to **1**, the corresponding chloride (**14a**) and nitrate (**14c**) salts were similarly obtained. The tetraphenyl borate salt (**14d**) was prepared from **14a** and $NaBPh_4$ in acetone. After evaporation of the solvent, the residue was crystallized from toluene–CH_2Cl_2.

By use of an essentially similar procedure, the following compounds were obtained by using complexes **4**, **11**, **12**, and **13** as starting materials: [Ni(C(NHBu^t)CH$_2$CMe$_3$)Cl(PMe$_3$)$_2$]BF$_4$ (**15**), yellow crystals; [CpNi(C(NHBu^t)Me)(PMe$_3$)]BF$_4$ (**16**), green crystals; [CpNi(C(NHBu^t)CH$_2$CMe$_2$Ph)(PMe$_3$)]BF$_4$ (**17**), green crystals; [Ni(C(NHBu^t)Me)(S$_2$CNMe$_2$)(PMe$_3$)]BF$_4$ (**18**), yellow-brown crystals, respectively.

Deprotonation of Complex 14b. A suspension of **14b** (0.34 g, 0.9 mmol) in a mixture of Et_2O–THF (1:1, 30 mL) was cooled at -60 °C, and NaCp was added (0.9 mL of a 1 M solution in THF) via syringe. After 3 h of stirring at room temperature, the volatiles were removed in vacuo, and the residue was extracted with a mixture of petroleum ether–Et_2O. Centrifugation, partial removal of the solvent, and cooling at -30 °C furnished compound **1** in 60% yield.

Deprotonation with powdered NaOH could also be effected, but workup of the reaction is difficult due to side reactions that afford hydroxo complexes of nickel.

Acknowledgment. Generous support of this work by the Dirección General de Política Científica is very gratefully acknowledged.

Electronic Structure of the Nonclassical Trimetallic Alkyne Cluster Complex $Os_3(CO)_9(\mu\text{-}H)_2(\mu_3\text{-}HC_2NEt_2)$

Zafiria Nomikou, Jean-François Halet,† and Roald Hoffmann*

Department of Chemistry and Materials Science Center, Cornell University, Ithaca, New York 14853

James T. Tanner and Richard D. Adams

Department of Chemistry, University of South Carolina, Columbia, South Carolina 29208

Received May 31, 1989

The electronic structure of the new 48-electron basketlike cluster compound $Os_3(CO)_9(\mu\text{-}H)_2(\mu_3\text{-}HC_2NEt_2)$ is compared to that of 46-electron closo and 48-electron nido M_3C_2 complexes. The unusual coordination of the alkyne ligand is attributed to the diethylamino group linked to one of the carbon atoms of the alkyne moiety.

To date, trimetallic alkyne cluster complexes have been encountered in two distinct geometries separated by their electron counts. Those characterized by 46 cluster valence electrons (CVE's), or 6 skeletal electron pairs (SEP's),[1] adopt a closo trigonal-bipyramidal structure (**1**) with the alkyne moiety lying perpendicular to one metal–metal bond. The others, possessing 48 CVE's or 7 SEP's, describe a nido square-pyramidal geometry (**2**), the acetylenic ligand positioned parallel to a metal–metal vector. In each case the neutral acetylene is counted as a 4-electron ligand. The recent synthesis and structure determination by two

† Permanent address: Laboratoire de Chimie du Solide et Inorganique Moléculaire, URA 254, Université de Rennes I, 35042 Rennes-Cédex, France.

(1) (a) Wade, K. *J. Chem. Soc. D.* **1971**, 792. (b) Mingos, D. M. P. *Nature (London), Phys. Sci.* **1972**, *236*, 99.

0276-7333/90/2309-0588$02.50/0

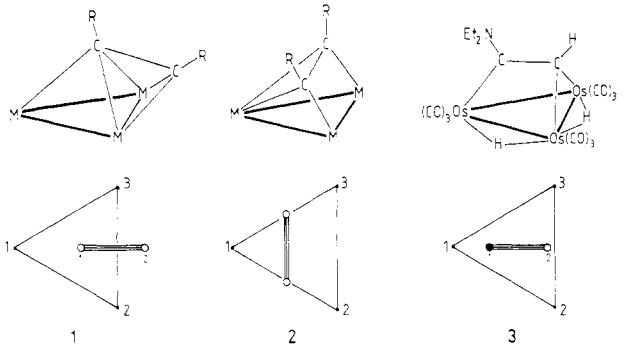

1 2 3

of us of the unusual 48-electron trimetallic alkyne compound $Os_3(CO)_9(\mu\text{-}H)_2(\mu_3\text{-}HC_2NEt_2)$[2] (**3**), having neither a closo nor a nido geometry, prompted us to study its electronic structure and to compare it with both 46-electron *closo*- and 48-electron *nido*-M_3C_2 clusters. To do this, extended Hückel calculations have been performed, with details provided in the Appendix.

Compound **3** contains a triangular osmium array with a triply bridging HC_2NEt_2 ligand lying perpendicular to an osmium–osmium vector, i.e. a μ_3-(η^2-$\perp$) coordination mode[3] characteristic of the 46-electron closo clusters such as $Fe_3(CO)_9(\mu_3\text{-}C_2Ph_2)$.[4] However, the coordination of the alkyne moiety in **3** also differs significantly from the one in the 46-electron *closo*-M_3C_2 cluster since the ligand is shifted away from the perpendicular edge Os(2)–Os(3), so much so that the carbon atom bearing the diethylamino group is bonded only to Os(1) (see **3**). Thus, the ligand can appropriately be described as a (dimetallomethyl)-(diethylamino)carbene. The title compound can be viewed as a basketlike cluster with the three osmium atoms and one of the carbon atoms forming the basket framework and the other carbon atom, bearing the NEt_2 group, providing the handle. The particular shape of compound **3** is attributed to the presence of the diethylamino group in the alkyne ligand. Indeed, the carbon–nitrogen separation is rather short, 1.33 Å [1.307 Å][2b] (expected C–N single and double bonds are 1.47 and 1.27 Å, respectivley). The nitrogen atom is planar and the ethyl groups are nonequivalent by ^1H NMR spectroscopy, due to the hindered rotation about the C–N bond.[2] Note that the two carbon atoms of the ethyl groups linked to the nitrogen atom lie in the plane defined by N, C(1), C(2), and H, almost perpendicular to the Os_3 plane. The partial double bond between C and N must somehow prevent the C atom from binding to more than one metal atom of the triangle. The asymmetry in the carbon–metal separations in **3** (Os(2)–C(1), 2.91 Å [2.934 Å]; Os(3)–C(1), 2.80 Å [2.807 Å]; Os(2)–C(2), 2.17 Å [2.173 Å]; Os(3)–C(2), 2.14 Å [2.144 Å]) is attributed to the hydrogen atoms bridging the Os(1)–Os(2) and Os(2)–Os(3) vectors. Significant asymmetry has also been observed in some *nido*-M_3C_2 clusters containing bridging hydrogen atoms.[5]

We commence with a description of the bonding in the model $[Os_3(CO)_9(C_2H_2)]^{2-}$ with alternative closo (**1**), nido (**2**), and basketlike (**3**) geometries. This is followed by an analysis of the π-donor effect of the NEt_2 group on the alkyne ligand. Finally, the role of a π-acceptor substituent on the alkyne moiety is briefly analyzed.

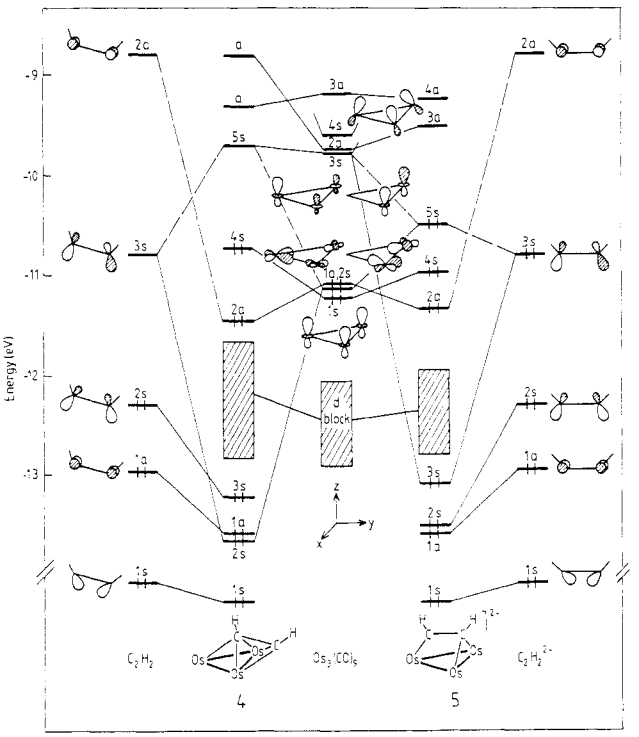

Figure 1. Interaction diagram of the model $Os_3(CO)_9(C_2H_2)$ in the 46-electron closo geometry (on the left) and the 48-electron basketlike geometry (on the right).

1. Comparison between Closo and Basketlike Structures of $[Os_3(CO)_9C_2H_2]^{2-}$

The electronic structure of the *closo*-M_3C_2 structure (**1**) has been extensively studied previously.[6] Therefore, we discuss it only briefly by showing the molecular orbital diagram of the closo model $Os_3(CO)_9(\mu_3\text{-}C_2H_2)$ (**4**), of symmetry C_s, on the left-hand side of Figure 1. The molecular orbitals of **4** shown in Figure 1, labeled s (symmetric) or a (antisymmetric) with respect to the mirror plane of the molecule, result from the interaction of the six frontier molecular orbitals (FMO's) of the triosmium moiety with the five FMO's ($\sigma + \pi + \pi^*$) of the acetylenic fragment. A gap of 1.04 eV separates the 4s HOMO from the 5s LUMO, securing reasonable stability of the closo system **4** for the expected count of 46 CVE's or 6 SEP's. The 6 skeletal electron pairs correspond to the 6 labeled occupied MO's, 4 of s and 2 of a symmetry, shown on the left-hand side of Figure 1.

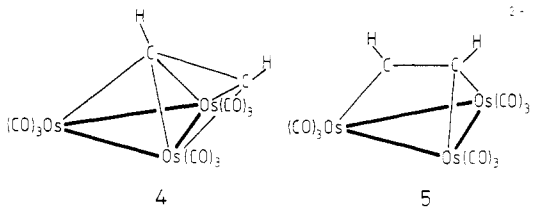

4 5

The effect of shifting of the alkyne ligand C_2H_2 away from the spanned Os(2)–Os(3) vector toward the other osmium atom Os(1) is illustrated on the right-hand side

(2) (a) Adams, R. D.; Tanner, J. T. *Organometallics* **1988**, *7*, 2241. (b) The same structure has also been reported by: Deeming, A. J.; Kabir, S. E.; Nuel, D.; Powell, N. I. *Organometallics* **1989**, *8*, 717. Distances given in brackets in the text refer to Deeming's structure.

(3) Thomas, M. G.; Muetterties, E. L.; Day, R. O.; Day, V. W. *J. Am. Chem. Soc.* **1976**, *98*, 4645.

(4) Blount, J. F.; Dahl, L. F.; Hoogzand, C.; Hübel, W. *J. Am. Chem. Soc.* **1966**, *88*, 292.

(5) Goudsmit, R. J.; Johnson, B. F. G.; Lewis, J.; Raithby, P. R.; Rosales, M. J. *J. Chem. Soc., Dalton Trans.* **1983**, 2257.

(6) (a) Schilling, B. E. R.; Hoffmann, R. *J. Am. Chem. Soc.* **1979**, *101*, 3456. (b) Granozzi, G.; Tondello, E.; Casarin, M.; Aime, S.; Osella, D. *Organometallics* **1983**, *2*, 430. (c) Halet, J.-F.; Saillard, J.-Y.; Lissillour, R.; McGlinchey, M. J.; Jaouen, G. *Inorg. Chem.* **1985**, *24*, 218. (d) Busetti, V.; Granozzi, G.; Aime, S.; Gobetto, R.; Osella, D. *Organometallics* **1984**, *3*, 1510. (e) Aime, S.; Bertoncello, R.; Busetti, V.; Gobetto, R.; Granozzi, G.; Osella, D. *Inorg. Chem.* **1986**, *25*, 4004.

of Figure 1, where we have shown the molecular orbital diagram of the basketlike model $[Os_3(CO)_9(\mu_3\text{-}C_2H_2)]^{2-}$ (**5**). Note the right-hand side of Figure 1 has two more electrons, i.e. one more occupied orbital, than the left side. The symmetry point group C_s is the same for the two structures **4** and **5**. Moreover, the alkyne ligand lies in the mirror plane in both cases. Thus, the symmetry labels of the FMO's of the frozen metallic triangle and the C_2H_2 ligand are identical in the closo (**4**) and the basketlike (**5**) geometries. The only change is the position of the acetylenic moiety with respect to the trimetallic entity. The major difference between the two structures **4** and **5** is the position of the 5s MO in the orbital diagram. This orbital is the LUMO of the 46-electron cluster and the HOMO of the 48-electron one. In the closo case (**4**), this orbital is rather high in energy, is vacant, and constitutes the LUMO of the complex. In **5**, the basketlike structure, this orbital lies at lower energy, close to the occupied 4s and 2a MO's. Now, a HOMO–LUMO gap of 1.01 eV exists in **5** if the 5s MO is occupied, favoring a total count of 48 CVE's or 7 SEP's. This is in agreement with the observed electron count of **3**. The seven labeled occupied MO's shown on the right-hand side of Figure 1 correspond to the seven SEP's characterizing the basketlike structure **5**.

Let us add two electrons to **4** and compare its total energy to that of **5**. The basketlike structure **5** is favored by 1.41 eV.[7] A close examination of the results indicates that this stabilization of **5** against **4** comes mainly from the 5s MO in **5**, 0.83 eV lower than in **4**. Why then is the 5s MO sufficiently low in energy in **5** to be populated?

In both cases, **4** and **5**, the 5s MO is, to a first approximation, one of the three MO's resulting from the interaction of one FMO of the alkyne ligand, 3s, with the two 2s and 3s FMO's of the metallic entity. These three FMO's considered are relatively close in energy, so their interaction will be determined mainly by their overlap. In the basketlike case **5**, the major interaction occurs between the metallic cluster 3s FMO and the 3s FMO of the alkyne moiety. Thus, the C_2H_2 3s orbital will be greatly stabilized after interaction and the Os_3 3s orbital largely destabilized. The Os_3 2s orbital remains almost unperturbed at rather low energy and constitutes the HOMO of the 48-electron complex **5**. This is depicted in **6**. In the closo case **4**, this

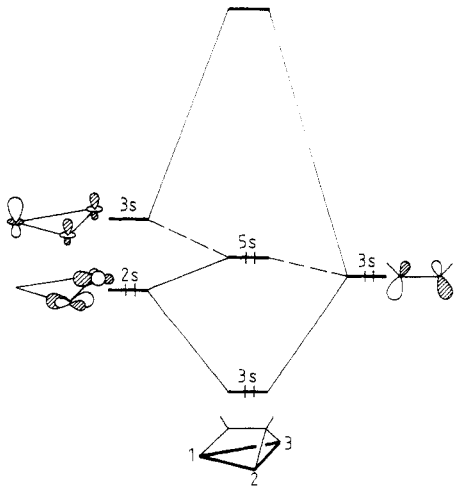

6

time the 3s orbital of the acetylenic fragment interacts mainly with the metallic 2s orbital and therefore is stabilized while the metallic 2s orbital is destabilized (see **7**).

(7) The different geometries were not optimized.

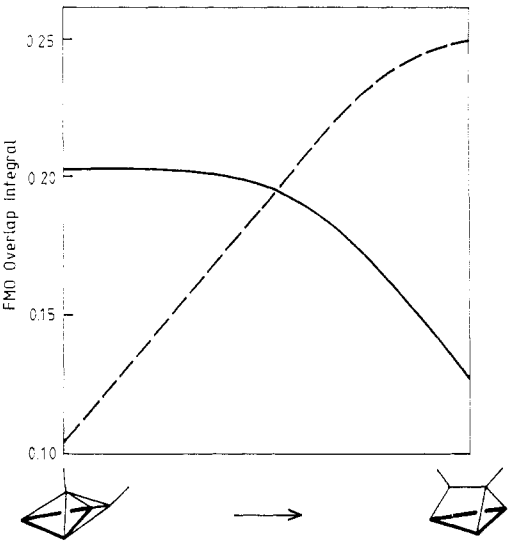

Figure 2. FMO overlap integrals $\langle 2s(Os_3)|3s(ac)\rangle$ (solid line) and $\langle 3s(Os_3)|3s(ac)\rangle$ (dashed line) plotted as a function of the slipping of the acetylenic ligand from **4** to **5**.

Finally, the metallic 3s orbital stays almost unchanged in energy and is the LUMO of the 46-electron closo complex **4**.

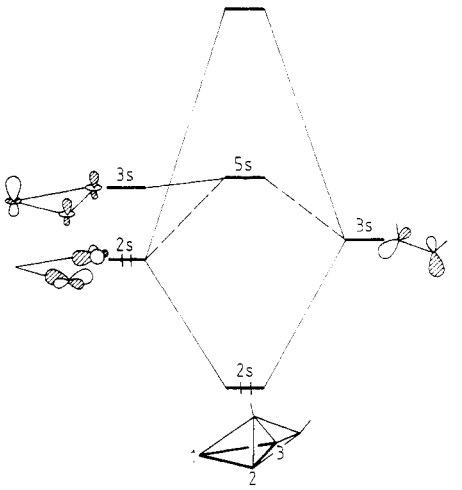

7

This analysis reveals that the slipping of the acetylenic ligand from the perpendicular Os(2)–Os(3) edge toward Os(1) is mainly due to a decrease of the overlap between the acetylenic π^* 3s FMO with the metallic in-plane 2s FMO localized preferentially on Os(2) and Os(3) and an increase of the overlap of the same C_2H_2 3s FMO with the metallic out-of-plane 3s FMO localized principally on Os(1). This is shown in Figure 2, where the FMO overlap integrals $\langle 2s(Os_3)|3s(ac)\rangle$ and $\langle 3s(Os_3)|3s(ac)\rangle$ have been plotted as a function of the slipping of the acetylenic ligand from **4** to **5**.

2. Comparison between Basketlike and Nido Structures of $[Os_3(CO)_9(C_2H_2)]^{2-}$

The most important question arising is as follows: What is the stability of the 48-electron basketlike structure relative to that of the expected 48-electron nido complex? Our extended Hückel calculations on the model $[Os_3(CO)_9(C_2H_2)]^{2-}$ show the nido complex **8** to be preferred by 0.49 eV.[8] Moreover, the HOMO–LUMO energy gap increases markedly from 1.01 eV in the basketlike case to

(8) See ref 6 for a detailed study on *nido*-M_3C_2 clusters.

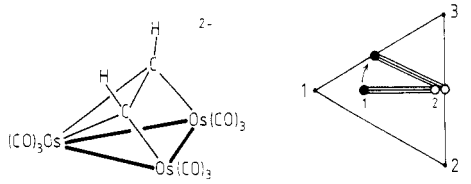

8 9

1.49 eV in the nido case. A second-order Jahn–Teller distortion is suspected in the basketlike structure **5**. This might lead to the more stable nido geometry **8**. Indeed, as drawn in **9**, only a small "windshield wiper" motion of 30° is sufficient to move from one geometry to the other.

The HOMO–LUMO regions of the basketlike (**5**) and the nido (**8**) structures are compared in Figure 3. Note that in order to keep the mirror plane in the ($y0z$) plane in both cases the alkyne ligand was "rotated" by 90° between **5** and **8**. The "90°" geometry is, of course, equivalent by symmetry to the "30°" one. The energies of the HOMO's of the two complexes are almost identical. The 3a LUMO of the basketlike structure is the middle orbital of a three-orbital mixing pattern arising from the interaction of the metallic 2a FMO with the acetylenic π 1a and π^* 2a FMO's. The destabilization of the metallic 2a orbital due to its interaction with the low-lying acetylenic π 1a orbital is counterbalanced by a stabilization due to its interaction with the acetylenic π^* 2a orbital lying above. Thus, the metallic 2a orbital changes only slightly in energy after interaction. The same kind of three-orbital mixing is observed in the nido case **8**, but this time it occurs between the metallic 2a FMO and the two π^* orbitals of the acetylenic moiety, since the rotation of the C_2H_2 ligand induces a change in symmetry labels for its orbitals. The lowest π^* orbital, symmetric in **5**, is now antisymmetric in **8** with respect to the mirror plane, while the reverse situation occurs for the lowest π orbital. Though they have a rather different shape (see Figure 3), the overlap of the π 1a FMO with the metallic 2a FMO in **5** is almost identical with that of the π^* 1a FMO with the same metallic 2a orbital in **8** (0.22 vs 0.19). However, the acetylenic π^* orbital is closer to the metallic 2a orbital in energy. Therefore, a stronger interaction follows in **8** and the metallic 2a orbital is largely destabilized, giving the MO labeled "3a" on the right-hand side of Figure 3. The stabilization due to its interaction with the upper lying π^* 2a FMO is not sufficient to prevent it from being pushed up in energy. The LUMO of **8** is now the MO labeled "4a" in Figure 3, which is derived purely from the metallic in-plane antibonding 3a FMO.[6] Note the quotation marks in our notation. "3a" at the right is similar to 3a at the left, and "4a" at right is very much like 4a at the left. To label them correctly in order of increasing energy (i.e. call "3a" 4a and "4a" 3a) would cause some confusion. One does not need to worry about the noncrossing rule here. That most useful rule applies to the evolution of orbitals along some geometrical coordinate; in the present case a line connecting two orbitals signifies only descent, parentage, or strong contribution.

Both opening of the HOMO–LUMO gap and energy stabilization (0.49 eV, difficult to trace) explain the preference of the model $[Os_3(CO)_9(C_2H_2)]^{2-}$ for a nido geometry.

3. Effect of the NEt_2 Group in Basketlike and Nido Structures

We substituted the hydrogen atom on C(1) (filled circle in **3** and **9**) by an NH_2 amino group lying in the plane perpendicular to the osmium triangle and again performed

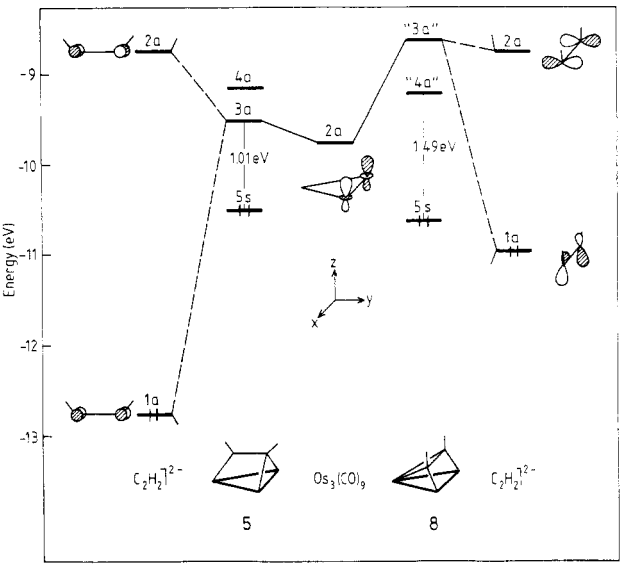

Figure 3. HOMO–LUMO region in the basketlike (on the left) and the nido (on the right) geometries of $[Os_3(CO)_9(C_2H_2)]^{2-}$. The mirror plane was kept in the ($y0z$) plane in both cases.

calculations on the basketlike and the nido structures. Our results yield the correct structural trend since the basketlike geometry is now preferred by 0.25 eV (remember that the unsubstituted basketlike model was less stable than the nido one by 0.49 eV). The HOMO–LUMO gap goes up from 1.01 eV in **5** to 1.35 eV in the substituted basketlike model $[Os_3(CO)_9(HC_2NH_2)]^{2-}$ (**10**), close to the 1.47 eV observed in the substituted nido complex **11**.

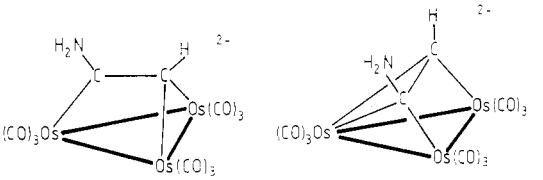

10 11

The effect of the π-donor NH_2 group on the alkyne ligand may be seen on the left-hand side of Figure 4. Replacement of one hydrogen atom by the amino group modifies the shape and the energy of the frontier orbitals, particularly the set of orbitals of a symmetry. Both π 1a and π^* 2a orbitals are pushed up in energy by interaction with the low-lying lone-pair p_x orbital of the nitrogen atom. Orbital 1a is then mainly localized on the unsubstituted C(2) atom (61%), while the upper lying π^* 2a orbital has an important contribution to the substituted C(1) atom (57%). These two orbitals form the recognizable second and third orbitals of an allylic π system. The nitrogen lone pair, lowest in energy, completes the set. The energy of the s frontier orbitals does not vary much, though their shape changes somewhat. Orbital 2s is localized preferentially on C(2) and 3s on C(1).

The interaction diagram for the substituted basketlike model **10** is shown on the right-hand side of Figure 5. The MO diagram of **5**, $[Os_3(CO)_9(C_2H_2)]^{2-}$, has been recalled on the left-hand side of the figure for comparison. Both diagrams resemble each other strikingly, except in the LUMO region. The 3a MO, the LUMO, in **5**, is pushed up in energy in the substituted basketlike complex **10**. As noted above, the metallic 2a FMO is localized principally on the Os(2) and Os(3) atoms. The rather strong overlap of the acetylenic 1a orbital with the metallic 2a FMO occurs between C(2) and Os(2) and Os(3). Therefore, it is not perturbed by the diminution of the contribution of

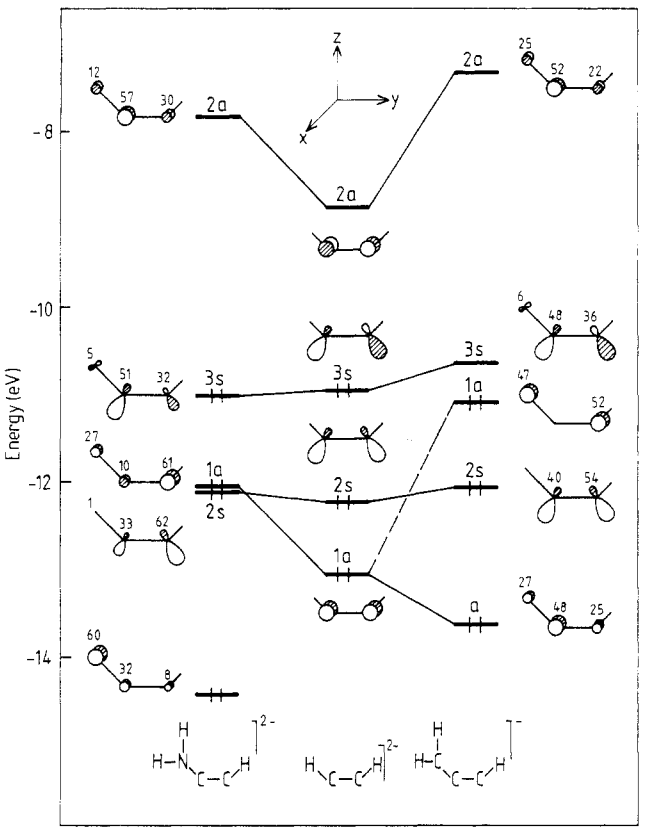

Figure 4. Frontier orbitals of the acetylenic ligand $[C_2H_2]^{2-}$, the aminoalkyne ligand $[HC_2(NH_2)]^{2-}$, and the allenyl ligand $[HC_2(CH_2)]^-$ (the numbers indicate the percentage of carbon character).

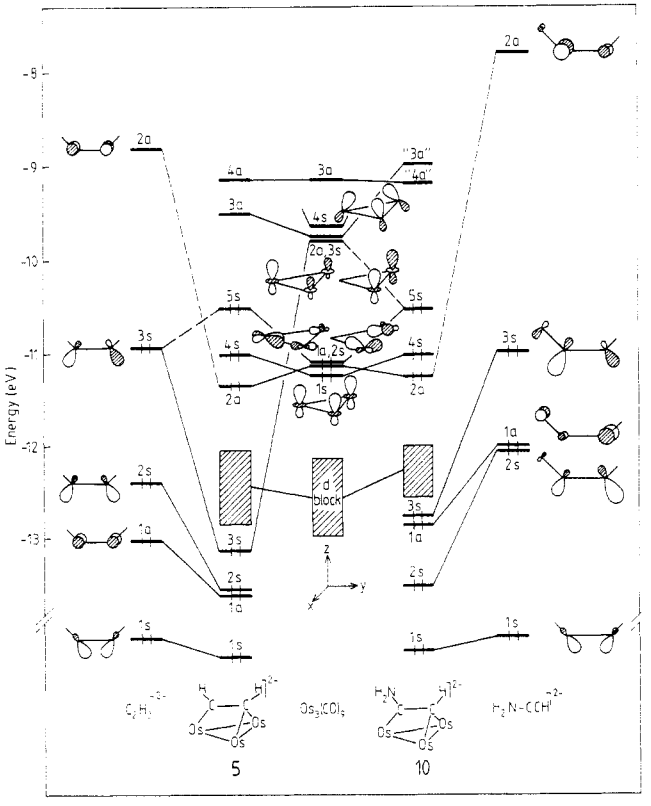

Figure 5. Interaction diagram for the models $[Os_3(CO)_9(C_2H_2)]^{2-}$ (on the left) and $[Os_3(CO)_9(HC_2NH_2)]^{2-}$ (on the right) in the basketlike geometry.

the substituted C(1) atom in 1a (0.22 in both cases). Because of a better energy match in **10**, the interaction between the metallic cluster 2a and HC_2R (R = NH_2, H), 1a FMO's is larger in **10** than in **5**. The result is a greater destabilization of the metallic 2a orbital, giving the high-lying "3a" MO in the complex (see the right-hand side of Figure 5). Moreover, its counterbalancing interaction with the upper acetylenic 2a orbital is weaker in **10** than in **5**. Thus, the HOMO–LUMO gap in the substituted basketlike complex is not between the 5s and "3a" MO's but between the 5s MO and the unperturbed in-plane antibonding "4a" MO.[6] We think that the larger HOMO–LUMO gap observed in **10** is one of the reasons explaining the resistance to a further deformation toward the nido geometry.

A difference of 0.25 eV separating the substituted basketlike model **10** from the substituted nido one **11** is rather difficult to trace. Another way to approach the preference for **10** consists of looking for a possible destabilization of the nido structure when one H atom is replaced by an amino group. A glance at the overlap populations in the different models, gathered in **12**, is useful. According to

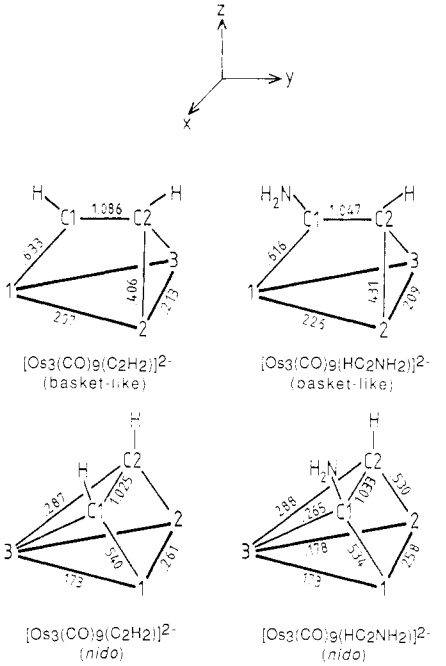

12

our calculations there is a tendency for weakening the bond between the substituted C(1) and Os(3) atoms in the nido complex $[Os_3(CO)_9(HC_2NH_2)]^{2-}$. The C(1)–Os(3) overlap population is 0.265 vs 0.288 between C(2) and Os(3). The difference, though weak, is noticeable, and the "windshield wiper" motion toward the basketlike structure could be facilitated.

Let us remark that the donor 3s and acceptor 2a frontier orbitals of the aminoalkyne ligand, mainly localized on C(1), are reminiscent of the occupied n(σ) and vacant n(π) orbitals of a CH_2 carbene ligand (see Figure 4). Therefore, the aminoalkyne moiety is expected to behave like a carbene ligand vis-à-vis Os(1) in **10**. Indeed, 0.73 electron is transferred from the 3s FMO of the aminoalkyne unit toward the metallic triangle, while 0.18 electron is back-donated into the aminoalkyne 2a FMO. This is in agreement with the description of the aminoalkyne ligand in the title compound as a (dimetallomethyl)(diethylamino)carbene.

An alternative fragmentation of the nido models $[Os_3(CO)_9(HC_2H)]^{2-}$ (**8**) and $[Os_3(CO)_9(HC_2NH_2)]^{2-}$ (**11**) into three entities, $Os_3(CO)_9$, C(1)–R (R = H, NH_2), and C(2)–H, is helpful in analyzing the weakening of the Os-

(3)–C(1) bond in **11**. In the nido case **8**, some bonding between Os(3) and C(1) occurs through the interaction of the p_y orbital of the CH groups with the occupied metallic FMO's (see **12** for the coordinate axes). The interaction is rather important, despite a poor overlap, because of a close energy match between interacting orbitals. When the H atom on C(1) is substituted by NH_2, this acetylenic p_y orbital is destablized by mixing with the low-lying lone pair of the N atom. Since it is farther removed in energy, its interaction with the occupied metallic FMO's is poorer in **11**. The occupation of this orbital after interaction is 0.85 electron in the substituted case, whereas it is 1.15 electrons in the unsubstituted one. That means this orbital, "busy" in the partial double bond between C(1) and N atoms, is less available for bonding with the metallic triangle. This favors the basketlike structure. Let us note that a lengthening of the C–N vector, i.e. toward a single bond, would stabilize the acetylenic p_y orbital, thus favoring the nido geometry over the basketlike one. This would imply some pyramidalization of the nitrogen atom and a slight shortening of the C–C bond. This is nicely illustrated in the following examples. Two triosmium aminoalkyne compounds have been characterized, namely the title complex $Os_3(CO)_9(H)_2(HC_2NEt_2)$[2] and $Os_3(CO)_9(H)_2(MeC_2NMe_2)$.[9] Although very similar, the aminoalkyne ligand in the latter is significantly twisted back toward the nido geometry and the C–N bond is substantially longer than the one observed in the former complex (1.40 vs 1.33 Å [1.307 Å]), while the C–C bond is almost unchanged (slightly shorter if compared to Deeming's compound[2b]): 1.43 vs 1.43 Å [1.459 Å].

Surprisingly, the presence of the amino group and a different coordination mode of the alkyne ligand in the basketlike complex $[Os_3(CO)_9(HC_2NH_2)]^{2-}$ does not affect the bonding between the two carbon atoms. In all our models the C(1)–C(2) overlap populations are comparable (see **12**). This is in agreement with the C–C separation of 1.43 Å [1.459 Å] observed in the title compound, in the same range as those reported in other Os_3C_2 compounds.[5,6e,10]

Finally, let us mention that substitution of an amino group on the C(2) atom in the basketlike geometry (open circle in **3** and **9**) gives a complex 0.73 eV less stable than **10**. This isomer, shown in **13**, is unlikely.

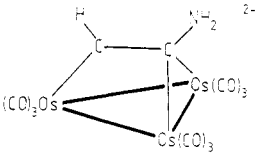

13

4. From Nido to Basket: The "Windshield Wiper" Motion

Several trimetallic alkyne complexes containing a π-donor substituent on the alkyne moiety have been structurally characterized and are listed in Table I. A glance at the $d_{M\text{-}C(R')}/d_{M\text{-}C(R)}$ ratio, corresponding to $d_{Os(3)\text{-}C(1)}/d_{Os(3)\text{-}C(2)}$ in **9**, shows that the deviation from the parallel mode (nido geometry) toward the slipped perpendicular model (basketlike geometry) becomes more and more important as the donor capabilities of the alkyne R′ substituent increase (OEt < NMe_2 < NEt_2).[13]

Table I. Structurally Characterized Trimetallic Substituted-Alkyne Complexes $M_3(CO)_9(\mu\text{-}H)_2(\mu_3\text{-}RC_2R')$

compd	$d_{M\text{-}C(R)}$, Å	$d_{M\text{-}C(R')}$, Å	$d_{M\text{-}C(R')}/d_{M\text{-}C(R)}$	ref
$Os_3(CO)_9(\mu\text{-}H)_2(C_6H_4)$	2.31	2.37	1.026	5
$Os_3(CO)_9(\mu\text{-}H)_2(\mu_3\text{-}HC_2OEt)$	2.32	2.45	1.056	11
$Ru_3(CO)_9(\mu\text{-}H)_2(\mu_3\text{-}MeC_2OMe)$	2.221	2.391	1.077	12
$Os_3(CO)_9(\mu\text{-}H)_2(\mu_3\text{-}C_4H_2S)$	2.23	2.46	1.103	20
$Os_3(CO)_9(\mu\text{-}H)_2(\mu_3\text{-}C_4H_2S)$	2.23 2.31	2.46 2.43	1.103 1.052	20
$Os_3(CO)_9(\mu\text{-}H)_2(\mu_3\text{-}C_4H_2NMe)$	2.24 2.24	2.56 2.50	1.143 1.116	20
$Os_3(CO)_9(\mu\text{-}H)_2(\mu_3\text{-}MeC_2NMe_2)$	2.25	2.62	1.164	9
$Os_3(CO)_9(\mu\text{-}H)_2(\mu_3\text{-}HC_2NEt_2)$	2.14 2.144	2.80 2.807	1.308 1.309	2a 2b

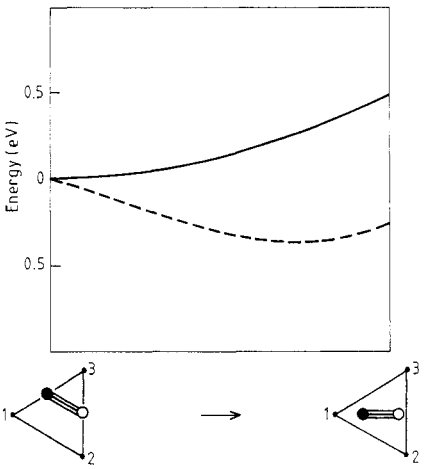

Figure 6. Total energy change for $[Os_3(CO)_9(C_2H_2)]^{2-}$ (solid line) and $[Os_3(CO)_9(HC_2NH_2)]^{2-}$ (dashed line) as a function of the slipping of the acetylenic moiety from a nido geometry to a basket geometry.

The total energy change as a function of the twisting of the alkyne ligand from the nido geometry to the basket geometry, depicted in **9**, is sketched in Figure 6 for the unsubstituted (solid line) and the substituted (dashed line) trimetallic alkyne complexes $[Os_3(CO)_9(HC_2R)]^{2-}$ (R = H, NH_2). As expected, the unsubstituted model favors the nido geometry. The energy curve for the substituted complex is almost flat and reveals a shallow and broad minimum for a basket geometry that is slightly unsymmetric, i.e. with a $d_{Os(2)\text{-}C(1)}/d_{Os(3)\text{-}C(1)}$ ratio (see **9**) not equal to 1 but to 1.07. This corresponds to the best FMO overlap compromise. Gratifyingly, the crystallographic data of the title compound exhibit a ratio of 1.04! All along the "windshield wiper rotation" process, HOMO–LUMO gap values over 1 eV were found, which are reasonable criteria

(9) Adams, R. D.; Chen, G.; Tanner, J. T. To be submitted for publication.

(10) (a) Pierpont, C. G. *Inorg. Chem.* **1977**, *16*, 636. (b) Clauss, A. D.; Shapley, J. R.; Wilson, S. R. *J. Am. Chem. Soc.* **1981**, *103*, 7387. (c) Henrick, K.; McPartlin, M.; Deeming, A. J.; Hasso, S.; Manning, P. *J. Chem. Soc., Dalton Trans.* **1982**, 899.

(11) Boyar, E.; Deeming, A. J.; Felix, M. S. B.; Kabir, S. E.; Adatia, T.; Bhusate, R.; McPartlin, M.; Powell, H. R. *J. Chem. Soc., Dalton Trans.* **1989**, 5. See also: (a) Byar, E.; Deeming, A. J.; Kabir, S. E. *J. Chem. Soc., Chem. Commun.* **1986**, 577. (b) Kaesz, H. D.; Jensen, C. M. *J. Organomet. Chem.* **1987**, *330*, 133.

(12) Churchill, M. R.; Fettinger, J. C.; Keister, J. B.; See, R. F.; Ziller, J. W. *Organometallics* **1985**, *4*, 2112.

(13) No twisting from the parallel mode is observed in the 47-electron compound $[Fe_3(CO)_9(\mu_3\text{-}MeC_2O)]^{2-}$, containing a propynolate anion ligand, $(MeC_2O)^-$. See: Dahan, F.; Mathieu, R. *J. Chem. Soc., Chem. Commun.* **1984**, 432.

for complex stability. These results are in agreement with the different characterized compounds gathered in Table I, adopting a range of structures between nido and basket. Deeming et al. have recently reported that there is a fine energetic balance between the basketlike and nido structures in $Os_3(CO)_9(H)_2(HC_2OEt)$,[2b] while the basketlike form for $Os_3(CO)_9(H)_2(HC_2NEt_2)$ was preferred by more than 0.25 eV over the nido one in our calculations.

The very soft potential energy profile shown in Figure 6 for the nido/basketlike interconversion of $[Os_3(CO)_9(HC_2NH_2)]^{2-}$ allows us to eliminate other possible pathways, particularly the one involving the unlikely complex **13** as an intermediate.

5. Effect of Introducing an Acceptor Group in Basketlike and Nido Structures

It is interesting to speculate about the effect of a very different type of substituent on the acetylene, a π-acceptor. We performed calculations on both basketlike and nido geometries in which the H atom borne by C(1) (see **9**) was replaced by the CH_2^+ cationic methylene ligand, a typical π-acceptor group.

The frontier orbitals of the allenyl group $[HC_2CH_2]^-$ are represented on the right-hand side of Figure 4. Except for the fact that the 3s FMO is vacant in the allenyl anion and occupied in the aminoalkyne dianion, the orbital sets of both ligands are strikingly comparable. The π-nonbonding 1a FMO's, which play an important role in the geometry preference, are almost identical, mainly localized on the unsubstituted carbon atom and the substituent atom of the alkyne moiety. Therefore, it is no surprise that the basketlike geometry is preferred against the nido one by 0.25 eV for the 48-electron cluster model $[Os_3(CO)_9(HC_2CH_2)]^-$. Here again, the substituted carbon atom, "busy" with the carbon atom of the CH_2^+ group in forming a partial double bond, is less available to bind to the metallic triangle. Examination of the overlap populations in nido and basketlike allenyl trimetallic models (see **14**) shows

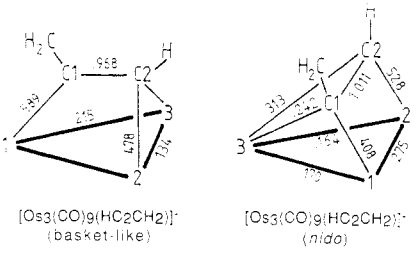

14

the same result as in the donor case, i.e. a weakening of the Os(3)–C(1) bond in the nido compound, favoring the basketlike structure. We also note in the same complex a rather large difference between Os(1)–C(1) and Os(2)–C(2) overlap populations (0.408 vs 0.528). Such a difference was not observed previously in the π-donor-substituted model **10** (0.534 vs 0.530). The LUMO of the nido complex $[Os_3(CO)_9(HC_2CH_2)]^-$ is chiefly the bonding combination of the metallic 2a orbital with the allenyl 2a FMO. In addition the $(HC_2CH_2)^-$ 1a orbital mixes into that orbital in an antibonding fashion to the metallic 2a FMO. This is sketched in **15**. The net result is that for

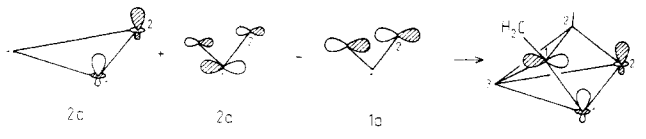

15

Table II. Extended Hückel Parameters

orbital	H_{ii}, eV	ζ_1	ζ_2	c_1^a	c_2^a
H 1s	−13.60	1.3			
C 2s	−21.40	1.625			
2p	−11.40	1.625			
N 2s	−26.00	1.950			
2p	−13.40	1.950			
O 2s	−32.30	2.275			
2p	−14.80	2.275			
Os 6s	−8.17	2.452			
6p	−4.81	2.429			
5d	−11.84	5.571	2.416	0.6372	0.5598

[a] Coefficients in the double-ζ expansion.

this level the Os(1)–C(1) overlap population is rather large (0.078), while the Os(2)–C(2) one is nearly zero. Therefore, occupation of this cluster MO would render almost equal the Os(1)–C(1) and Os(2)–C(2) total overlap populations (0.486 vs 0.528 calculated for $[Os_3(CO)_9(HC_2CH_2)]^{3-}$). This is what was happening for the nido model **11**, $[Os_3(CO)_9(HC_2NH_2)]^{2-}$.

The calculated HOMO–LUMO gap in both nido and basketlike structures, ca. 0.50 eV, is not very impressive. Bending of the CH_2 group toward one metal atom and coupled rearrangement of the cluster are usually observed in 48-electron allenyl trimetallic compounds, presumably in order to stabilize them and satisfy their electronic requirements.[14] Note here also that the basketlike isomer with the CH_2^+ group linked to C(2) (see **9**) is unlikely, being 1.33 eV less stable than the other basketlike isomer.

6. Conclusion

We feel that there is a competition between the basketlike and the nido geometries. They are very close in energy to each other. An interconversion between a basketlike structure with a short, nearly double, C–N bond length and a nido structure with a single C–N bond does not seem out of the question. We may ask if the title compound would be observed in the closo geometry (**1**) with two electrons less. Calculations on the 46-electron closo model $Os_3(CO)_9(HC_2NH_2)$ give the isomer with the amino group linked to C(2) (see **1**) to be the most stable but show some weakening of the Os–C(2) bonds compared to those in the unsubstituted closo complex. Thus, the presence of an amino group in a closo 46-electron compound might induce lengthening of some metal–carbon bonds if such a complex exists.

The results obtained from this study are also valid for the 50-electron trimetallic alkyne clusters. The trimetallic aminoalkyne compound $Os_3(CO)_9(\mu_3\text{-}S)(\mu_3\text{-}MeC_2NMe_2)$ has a basketlike structure with an open metallic triangle,[15] while the cluster $Ru_3(CO)_9(\mu_3\text{-}S)(\mu_3\text{-}HC_2Ph)$ adopts the expected nido geometry of a pentagonal M_3SC_2 pyramid.[16]

Acknowledgment. We thank Professor J.-Y. Saillard for helpful comments. The stay of J.-F.H. at Cornell University was made possible by a grant from a 1987–1988 NSF-CNRS Exchange Program. Thanks are expresed to Louis Hubert for the drawings. Our work at Cornell was supported by Research Grants CHE 8406119 and DMR 8516616-A02 from the National Science Foundation.

(14) See for example: (a) Aime, S.; Osella, D.; Arce, A. J.; Deeming, A. J.; Hursthouse, M. B.; Galas, A. M. R. *J. Chem. Soc., Dalton Trans.* **1984**, 1981 and references therein. (b) Adams, R. D.; Tanner, J. T. *Organometallics* **1989**, *8*, 563.

(15) Adams, R. D.; Chen, G.; Tanner, J. T.; Yin, J. *Organometallics* **1989**, *8*, 2493.

(16) Adams, R. D.; Babin, J. E.; Tasi, M.; Wolfe, T. A. *Organometallics* **1987**, *6*, 2228.

Appendix

All calculations have been carried out within the extended Hückel formalism[17] with use of the weighted H_{ij} formula.[18] The atomic parameters utilized are listed in Table II. The parameters for Os come from earlier work.[19] In all models one axial and two equatorial carbonyls were terminally bonded to each Os atom and the following bond distances (Å) were used: Os-Os = 2.85, Os-C(O) = 1.92, C-O = 1.15, C-C = 1.43, C-N = 1.33, C-H = 1.09, N-H = 1.01. All the C(O)-Os-C(O) angles were set at 90°. In the closo models, Os-C(1) and Os(2,3)-C(2) distances were set equal to 2.15 and 2.10 Å, respectively, whereas in the basketlike models Os(1)-C(1) = 2.10 Å and Os(2,3)-C(2) = 2.15 Å. Finally, in the nido complexes, Os(1)-C(1,2) and Os(2,3)-C(1,2) distances of 2.15 and 2.10 Å, respectively, were used.

Registry No. 3, 105286-41-7.

(17) Hoffmann, R. *J. Chem. Phys.* **1963**, *39*, 1397.
(18) Ammeter, J. H.; Bürgi, H.-B.; Thibeault, J. C.; Hoffmann, R. *J. Am. Chem. Soc.* **1978**, *100*, 3686.
(19) Jørgensen, K. A.; Hoffmann, R. *J. Am. Chem. Soc.* **1986**, *108*, 1867.
(20) Deeming, A. J.; Arce, A. J.; De Sanctis, Y.; Day, M. W.; Hardcastle, K. I. *Organometallics* **1989**, *8*, 1408.

Cluster Complexes Containing Ynamine Ligands. 2. Reactions of $MeC{\equiv}CNMe_2$ with $M_3(CO)_{10}(\mu_3\text{-}S)$ (M = Fe, Ru, Os) and Structural Characterizations of $Ru_2(CO)_6[\mu\text{-}SC(NMe_2)CMe]$, $Ru_2(CO)_6[\mu\text{-}SCMeC(NMe_2)]$, and $Os_3(CO)_9[\mu_3\text{-}MeC_2NMe_2](\mu_3\text{-}S)$

Richard D. Adams,* Gong Chen, James T. Tanner, and Jianguo Yin

Department of Chemistry, University of South Carolina, Columbia, South Carolina 29208

Received September 22, 1989

The reactions of the compounds $M_3(CO)_{10}(\mu_3\text{-}S)$ (**1a**, M = Fe; **1b**, M = Ru) with MeC_2NMe_2 yielded the products $M_2(CO)_6[\mu\text{-}SC(NMe_2)CMe]$ (**2a**, M = Fe, 3%; **2b**, M = Ru, 36%) and $M_3(CO)_9[\mu_3\text{-}MeC_2NMe_2](\mu_3\text{-}S)$ (**3a**, M = Fe, 30%; **3b**, M = Ru, 14%). The reaction of $Os_3(CO)_{10}(\mu_3\text{-}S)$ (**1c**) with MeC_2NMe_2 yielded only the trinuclear product $Os_3(CO)_9[\mu_3\text{-}MeC_2NMe_2](\mu_3\text{-}S)$ (**3c**, 87%). Compounds **2b** and **3c** were characterized by single-crystal X-ray diffraction analyses. Compound **2b** consists of a metal-metal-bonded $Ru_2(CO)_6$ grouping bridged by a $SC(NMe_2)CMe$ ligand. The sulfur and *C*-methyl carbon atom are strongly bonded to both metal atoms. The NMe_2-substituted carbon atom is weakly bonded to one metal atom and not bonded to the other. Compound **3c** consists of an open triosmium cluster with a triply bridging sulfido ligand and a triply bridging MeC_2NMe_2 ligand. The *C*-methyl carbon atom is bonded to two metal atoms. The NMe_2-substituted carbon atom is coordinated only to the one remaining metal atom. Structurally, this grouping resembles an NMe_2-substituted carbene ligand. This is also supported by the ^{13}C NMR spectrum, which shows a very low field resonance, +251.92 ppm for **3a** and +243.50 ppm for **3c**. It is proposed that the ynamine ligands in the compounds **3a-c** should be formulated as (α,α-dimetallioethyl)(dimethylamino)carbene ligands. Compound **2b** isomerizes when heated to form the compound $Ru_2(CO)_6[\mu\text{-}SC(Me)CNMe_2]$ (**2b'**) in 38% yield. Compound **2b'** was characterized structurally. The structure is similar to that of **2b** except that the methyl-substituted carbon atom is bonded to the sulfur atom and the NMe_2-substituted carbon atom is not a bridging atom but is terminally coordinated to one of the metal atoms. The iron homologue of **2b'**, $Fe_2(CO)_6[\mu\text{-}SC(Me)CNMe_2]$ (**2a'**), was obtained (55% yield) by pyrolysis of **3a** at 100 °C. Crystal data: for **2b**, space group $P\bar{1}$, a = 9.189 (1) Å, b = 11.705 (3) Å, c = 8.213 (1) Å, α = 106.18 (1)°, β = 110.06 (1)°, γ = 79.60 (2)°, V = 793.3 (3) Å^3, Z = 2, R = 0.020, and R_w = 0.023 for 2373 reflections; for **2b'**, space group $P2_1/n$, a = 10.531 (2) Å, b = 10.799 (2) Å, c = 14.336 (3) Å, β = 98.07 (2)°, V = 1614 (1) Å^3, Z = 4, R = 0.025, and R_w = 0.026 for 1615 reflections; for **3c**, space group $P\bar{1}$, a = 9.397 (4) Å, b = 13.406 (7) Å, c = 8.914 (3) Å, α = 92.84 (4)°, β = 115.20 (3)°, γ = 97.54 (4)°, V = 1000.3 (8) Å^3, Z = 2, R = 0.030, and R_w = 0.035 for 2814 reflections.

Introduction

Recent studies of the ligand behavior of unsymmetrical ynamines, $RC{\equiv}CNR'_2$, have shown that these molecules exhibit unusual bridging coordinations.[1-5] In binuclear coordination, simple alkynes usually exhibit either the perpendicular (A) or parallel (B) bonding modes,[6] but

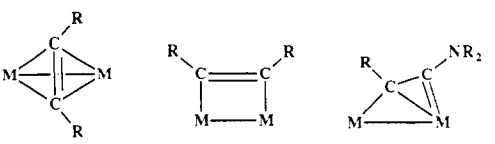

unsymmetrical ynamines have been found to exhibit the skewed bridging form C that lies approximately halfway

(1) Cabrera, E.; Daran, J. C.; Jeannin, Y.; Kristiansson, O. *J. Organomet. Chem.* **1986**, *310*, 367.
(2) Muller, F.; van Koten, G.; Kraakman, M. J.; Vrieze, K.; Heijdenrijk, D.; Zoutberg, M. C. *Organometallics* **1989**, *8*, 1331.
(3) Adams, R. D.; Tanner, J. T. *Organometallics* **1989**, *8*, 563.
(4) Adams, R. D.; Tanner, J. T. *Organometallics* **1988**, *7*, 2241.
(5) Deeming, A. J.; Kabir, S. E.; Nuel, D.; Powell, N. I. *Organometallics* **1989**, *8*, 717.
(6) Hoffman, D. M.; Hoffmann, R. *J. Chem. Soc., Dalton Trans.* **1982**, 1471.

0276-7333/90/2309-0595$02.50/0